



Impact of Flux Wire Selection on Neutron Spectrum Adjustment

August 2021

T. Holschuh and W. Windes
Idaho National Laboratory

J. Navarro and A. Conant
Oak Ridge National Laboratory



*INL is a U.S. Department of Energy National Laboratory
operated by Battelle Energy Alliance, LLC*

DISCLAIMER

This information was prepared as an account of work sponsored by an agency of the U.S. Government. Neither the U.S. Government nor any agency thereof, nor any of their employees, makes any warranty, expressed or implied, or assumes any legal liability or responsibility for the accuracy, completeness, or usefulness, of any information, apparatus, product, or process disclosed, or represents that its use would not infringe privately owned rights. References herein to any specific commercial product, process, or service by trade name, trade mark, manufacturer, or otherwise, does not necessarily constitute or imply its endorsement, recommendation, or favoring by the U.S. Government or any agency thereof. The views and opinions of authors expressed herein do not necessarily state or reflect those of the U.S. Government or any agency thereof.

Impact of Flux Wire Selection on Neutron Spectrum Adjustment

**T. Holschuh and W. Windes
Idaho National Laboratory
J. Navarro and A. Conant
Oak Ridge National Laboratory**

August 2021

**Idaho National Laboratory
Advanced Reactor Technologies
Idaho Falls, Idaho 83415**

<http://www.art.inl.gov>

**Prepared for the
U.S. Department of Energy
Office of Nuclear Energy
Under DOE Idaho Operations Office
Contract DE-AC07-05ID14517**

Page intentionally left blank

INL ART Program

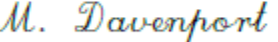
Impact of Flux Wire Selection on Neutron Spectrum Adjustment

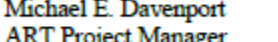
INL/EXT-21-64191
Revision 0

August 2021

Technical Reviewer: (Confirmation of mathematical accuracy, and correctness of data and appropriateness of assumptions.)


Austin C. Matthews 08/25/2021
Date

Approved by:

M. Davenport 8/25/2021
Date


Michael E. Davenport
ART Project Manager 8/25/2021
Date


Travis R. Mitchell
ART Program Manager 8/25/2021
Date


Michelle T. Sharp
INL Quality Assurance 8/24/2021
Date

EXECUTIVE SUMMARY

In reactor dosimetry, spectrum unfolding methods are used to assess the energy-dependent neutron flux following the irradiation of flux wires or foils. For some spectrum-unfolding methods, an *a priori*, or initial guess spectrum is necessary. However, if the *a priori* spectrum is not representative of the irradiation spectrum experienced by the flux wires, the spectrum-unfolding method may fail or create a nonphysical adjusted spectrum. The unfolded spectrum is dependent on flux-wire reaction rates and, therefore, cross-section. As a result, each selection or combination of flux wires will have a different sensitivity to the group-wise fluence difference between the *a priori* spectrum and the irradiation spectrum. Therefore, a selection of flux wires that are insensitive to errors in the *a priori* spectrum would be considered robust choices for reactor dosimetry. In this work, flux-wire reaction rates are calculated using a simulated neutron spectrum from the High Flux Isotope Reactor (HFIR) and spectrum-unfolding methods are used in each flux-wire combination. Flux-wire combinations are compared against a traditional flux-wire set of Ti, Fe, and Co, with a summary table of the deemed “good” wire combinations—i.e., those that are insensitive to number of *a priori* neutron-energy groups, group-wise difference between the *a priori* supposition and irradiation, and magnitude of difference.

Page intentionally left blank

CONTENTS

EXECUTIVE SUMMARY	iv
ACRONYMS.....	ix
1. INTRODUCTION.....	1
2. OBJECTIVES AND METHOD OF EVALUATION	3
2.1 Parametric Study Method of Evaluation	3
2.2 Computational Model of Energy-Dependent Neutron Flux.....	3
2.3 Flux-Wire Candidates	5
2.3.1 Nominal Flux-Wire Set.....	5
2.4 Flux Wire Reaction Rates	8
2.5 Spectrum Unfolding Algorithm – STAYSL	9
2.6 Comparison of Experimentally adjusted Neutron Flux.....	10
3. RESULTS AND DISCUSSION	11
3.1 Potential Large Deviation in <i>a priori</i> Spectrum.....	14
3.2 Well-Characterized, High-Confidence <i>a priori</i> Spectrum	14
4. REFERENCES.....	15

FIGURES

Figure 1. Flow of information for flux wire experiment and analysis	2
Figure 2. 640-group MCNP neutron spectrum with nominal, increased thermal, and increased fast contributions with large deviations from the nominal case	4
Figure 3. Spectrum unfolding for Co and Au with 640-group, small deviation <i>a priori</i> spectrum.	13
Figure 4. Spectrum unfolding for Co and Al with 640-group, small deviation <i>a priori</i> spectrum.	14

TABLES

Table 1. Neutron group strucutres and deviation from MCNP spectrum evaluated for this work.	4
Table 2. Parameters for Eq. (1).	6
Table 3. Chosen cases and number of STAYSL simulations performed.	6
Table 4. Materials and Reactions Used for Analysis [4, 16].	6
Table 5. Definition of variables for calculation of reaction rate from simulated data.	9
Table 6. Definition of variables for spectral adjustment [1].	10
Table 7. Results for potentially large deviation in <i>a priori</i> spectrum.	11
Table 8. Results for well-characterized, high-confidence <i>a priori</i> spectrum.	12
Table 9. List of ASTM standards relevant to reactor dosimetry.....	16

Page intentionally left blank

ACRONYMS

ASTM	American Society for Testing and Materials
ATR	Advanced Test Reactor
HFIR	High Flux Isotope Reactor
IRDFF	International Reactor Dosimetry and Fusion File
MCNP	Monte Carlo N-Particle
PT	pneumatic tube

Page intentionally left blank

Impact of Flux Wire Selection on Neutron Spectrum Adjustment

1. INTRODUCTION

Reactor dosimetry, or the assessment of energy-dependent neutron flux, is a powerful tool that can be used to validate computational tools as well as interpret dose to an experiment during irradiation. For a single experiment, many steps—shown in the flow path in Figure 1—must be achieved to perform a reactor-dosimetry measurement in accordance with American Society for Testing and Materials (ASTM) standards, such as those described in [1–3]. A full list of ASTM standards, practices, and guides relevant to reactor dosimetry are provided in Appendix A.

The steps in Figure 1 are listed below, with detailed information for each section. The arrows in Figure 1 depict the inputs and outputs that are required for each successive step in the flow path of the reactor dosimetry measurement.

1. Selection of Flux Wires
 - a. Improvements in reactor dosimetry are limited to isotopic reactions contained within the International Reactor Dosimetry and Fusion File (IRDFF) cross-section library [4].
 - b. The IRDFF consists of exclusively experimental data and contains many fast-neutron reactions to account for localized changes in fission spectrum (1–20 MeV) neutrons.
 - c. When selecting flux wires, it is typical to choose at least one neutron reaction that is sensitive to thermal neutron energies.
2. Neutron Irradiation of Flux Wires
 - a. The irradiation characteristics need to be known for an accurate reaction-rate determination, including irradiation duration.
3. Measurement of Flux Wires
 - a. The purpose of the flux-wire measurement is to quantify reaction rate for each potential reaction in the chosen flux wires.
 - b. Depending on the cooldown time between the end of irradiation and beginning of measurement, some activation products in the flux wires may have decayed below detectable limits.
 - c. The measurement may consist of one or more techniques:
 - i. Gamma spectrometry—Medium uncertainty (2–5%), easier to measure.
 - ii. Mass spectrometry—Low uncertainty (<1%), harder to measure, fewer facilities.
4. Computational Model of Energy-dependent Neutron Flux
 - a. The simulated *a priori* solution of neutron flux provides a first guess for some spectrum-unfolding algorithms.
 - b. If the *a priori* spectrum is substantially different from the true, experimental spectrum, some spectrum-unfolding algorithms can fail.
 - c. If the *a priori* spectrum is too coarse (few neutron groups), spectrum-unfolding algorithms become increasingly sensitive to differences between the *a priori* and the true experimental spectra.

- d. If the *a priori* spectrum is too coarse, spectrum-unfolding algorithms become increasingly sensitive to selection of flux wires, shown as dotted line in Figure 1.

5. Spectrum Unfolding Algorithm

 - a. Several software packages, including STAYSL PNNL [5, 6] and SAND-II[7], use a least-squares or logarithmic least-squares approach and use covariance data to assess total flux and energy-dependent flux uncertainties.
 - b. In particular, STAYSL incorporates the uncertainty in the *a priori* computational spectra [8, 9].
 - c. Custom packages are occasionally used for specific purposes [10–12].
 - d. Emerging approaches, such as genetic algorithms [13, 14], use other methodologies to interpret flux-wire reaction rates; however, flux uncertainty may be more difficult to quantify.

6. Experimentally Adjusted Energy-Dependent Neutron Flux

 - a. The output of each spectrum-unfolding algorithm provides an experimentally adjusted energy-dependent neutron flux that may then be used.
 - b. For this work, the experimentally adjusted neutron flux is compared to the computational model to assess the selection of the flux wires (blue arrow path).

7. Determination of Experiment Fluences of Interest

 - a. For some experiments, it may be of interest to determine a single energy equivalence, such as 1 MeV [15], which can be informally defined as the threshold for fast-neutron reactions and damage to materials such as graphite.

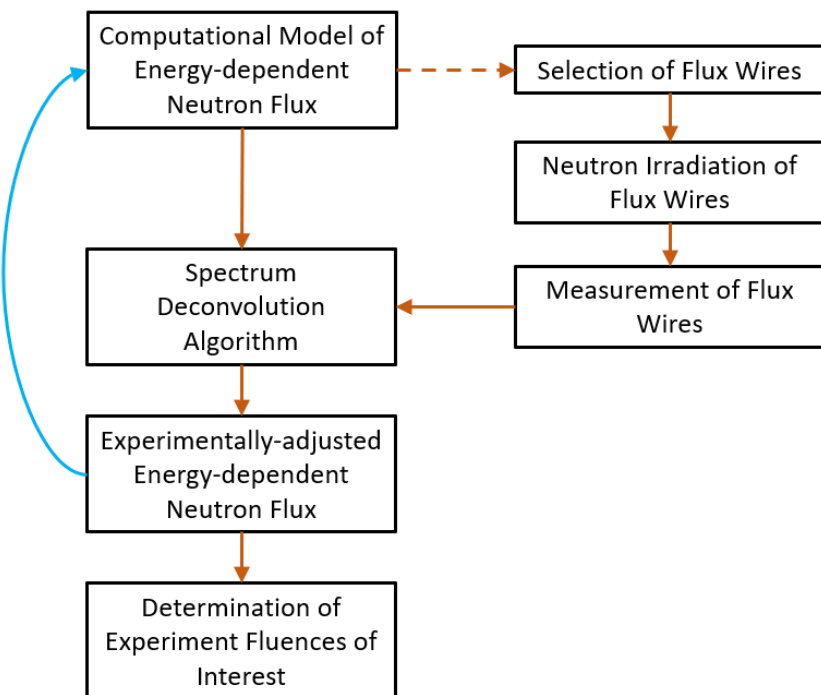


Figure 1. Flow of information for flux-wire experiment and analysis.

2. OBJECTIVES AND METHOD OF EVALUATION

The objective of this work is to determine an optimal selection of flux wires by evaluating the accuracy of the experimentally adjusted neutron energy spectrum following spectrum unfolding. The method of spectrum unfolding used in this work requires a computational “guess,” or *a priori*, spectrum as an initial starting point for calculation of the experimentally adjusted neutron spectrum.

There have been a number of previous works on reactor dosimetry and spectrum unfolding. However, no robust or parametric study on the sensitivity of the spectrum unfolding has been done to select flux wires or describe uncertainty in the *a priori* spectrum. Therefore, it is necessary to evaluate the impact of error in the *a priori* solution compared to the true spectrum that irradiates a flux wire. For example, will the spectrum-unfolding algorithm provide an accurate attribution of the irradiation flux if the *a priori* spectrum is given as a pure emitted-fission-neutron spectrum, but the true, irradiation spectrum is representative of a light-water-moderated spectrum with thermal- and epithermal-neutron populations?

This work represents an initial assessment because the variety of *a priori* and irradiation neutron spectra combinations are numerous. Thus, it is recommended that a reactor-dosimetry program assess its particular reactor spectrum type prior to experimental measurements for the determination of experimentally adjusted, energy-dependent neutron spectra.

2.1 Parametric Study Method of Evaluation

To directly address the computational tools within the steps of reactor dosimetry, the reaction rates of flux wires irradiated in HFIR’s pneumatic tubes (PTs) are simulated. The simulated reaction rates are calculated for all the available reactions within the IRDFF library.

The desired outcome is to determine a robust set of parameters that should govern a reactor-dosimetry experiment. For example, if a particular wire’s energy-dependent cross-section—and, therefore, reaction rate—causes instability in the spectrum unfolding with a small error/uncertainty in the *a priori* spectrum, that particular wire would not be suggested for future work in the reactor or experiment dosimetry project.

The three variables that are altered in each simulated reactor dosimetry end-to-end calculation are:

- Flux wires (choose combinations of two, three, or four wires)
- Number of neutron energy groups in the *a priori* neutron flux (100 or 640 groups)
- Adjustment of *a priori* spectrum (unchanged, increased thermal, and increased fast regimes).

2.2 Computational Model of Energy-Dependent Neutron Flux

The *a priori* spectrum was calculated using Monte Carlo N-Particle (MCNP) [17] in the HFIR PT-1 irradiation position. Two separate group structures, 100 and 640 groups, were used for the *a priori* spectrum, and two flux adjustments were performed. The flux adjustments intentionally manipulated the spectrum by either increasing or decreasing the thermal proportion of the reactor spectrum. However, the manipulations represent errors in the simulation environment and associated results, not changes in the irradiation spectrum. As a result, the saturated activities for each nuclear reaction were held consistent with the values from the simulated, unadjusted spectrum.

If the measured reaction rates are significantly different from the predicted reaction rates of the *a priori* spectrum, the adjusted spectrum following unfolding will not be accurate. In fact, due to the nature of the matrix solver within some unfolding algorithms, the resulting adjusted spectrum may be non-physical and have oscillating behavior, especially in the fast region.

One area of reactor dosimetry that is often misrepresented is the uncertainty in the simulated *a priori* spectrum. Stochastic solvers, such as MCNP, cannot fully represent the uncertainty in the calculated neutron flux though there are ongoing efforts to implement effective tools for stochastic uncertainty

determination in several different code packages. In previous work conducted at Idaho National Laboratory, the uncertainty-quantification tool [8, 9] shows that the uncertainty in a simulated MCNP spectrum for an Advanced Test Reactor (ATR) experiment is well within the realm of 5–10%. Localized changes in neutron flux due to neutron sources and sinks can easily be produced.

The presence of flux wires should not be viewed as a confirmation of the simulated neutron spectra. There are associated uncertainties as well as errors in nuclear data, and flux wires should be implemented as a mechanism for exposing the differences between simulation and experiments. If the simulation perfectly captures all relevant phenomena and geometry within a reactor experiment, the experimentally adjusted neutron spectrum would be exactly the same as the simulated neutron spectrum, and flux wires would be viewed, wrongly, as unnecessary. The neutron-group structures and deviations from the MCNP spectrum to be evaluated are shown in Table 1. The deviations are calculated as a logarithmic slope change from the nominal case. Figure 2 shows the 640-group structure with the nominal, increased thermal, and increased fast cases with large deviations to the MCNP nominal (true) spectrum.

Table 1. Neutron group structure and deviation from MCNP spectrum evaluated for this work.

Case	Neutron Group Structure	Deviation from MCNP (true) spectrum
A	640-group	Small (~5% at 1 MeV)
B	640-group	Large (~50% at 1 MeV)
C	100-group	Small (~5% at 1 MeV)
D	100-group	Large (~50% at 1 MeV)

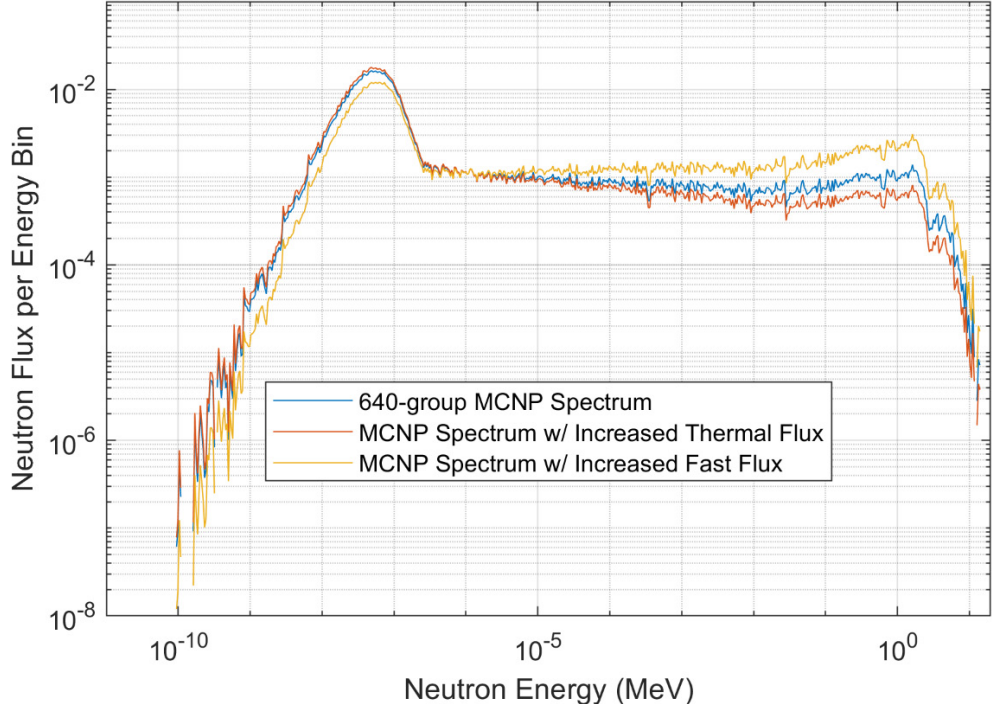


Figure 2. Six hundred and forty group MCNP neutron spectrum with nominal, increased thermal, and increased fast contributions with large deviations from the nominal case.

2.3 Flux-Wire Candidates

The term “wire” to illustrate a flux monitor is generalized in terms of this work. Foils and wires are traditionally the most-used shapes due to reduced wall thickness. A thick wire, or rod, would experience a decreased or modified neutron flux near the midline of the shape factor, and could inhibit accurate gamma spectrometry following irradiation due to photon attenuation through an optically translucent or opaque shape.

Additionally, foils can be made thin and positioned orthogonal to the flux to measure directional neutron flux. Then, a cadmium layer on one side of the foils allows for the measurement of neutron current.

The selection of a flux wire package is not solely dependent on its impact on a spectral adjustment. Chemical and physical properties of flux wire materials might preclude their use in reactor experiments. Additionally, half-lives of reaction products may be too short to provide useful information following irradiation. For example, many ATR experiments require long periods to be dismantled to retrieve flux wires. In other flux-wire materials, impurities may prevent the use of some materials. In a Ni flux wire, Co impurities can introduce ^{58}Co and ^{60}Co reaction products in addition to the concentrations of these radioisotopes from Ni. For all these reasons, it is imperative to maintain, produce, or purchase high-quality materials.

Thirty wires were chosen for analysis from the IRDFF cross-section library, with a total of 47 nuclear reactions. Fission and inelastic reactions were not included—for example, $^{235}\text{U}(\text{n},\text{f})$ or $^{93}\text{Nb}(\text{n},\text{n}')^{93m}\text{Nb}$. The thirty wires were combined with the change in spectrum adjustment and number of energy groups to create a large number of permutations and inputs for spectrum unfolding from the single irradiation spectrum. The possible flux wire combinations, Eq. (1), can be calculated for a number of unique wire combinations that can be created with a flux-wire package and a given number of available wires. The parameters for Eq. (1) are defined in Table 2 to calculate the number of combinations, C , which is then shown in Table 3 and is used to determine the total number of input files that will be used for spectrum unfolding. The flux-wire package was limited to four wires because of the number of permutations.

Table 4 provides the list of wires and isotope reactions chosen from the IRDFF cross-section library. Additionally, the threshold neutron energy for that reaction is shown, which is an approximate value from the IRDFF data. A null value indicates a thermal reaction or similar that does not have an energy threshold for the reaction.

Fast neutrons cause the most damage in irradiated materials. Therefore, the information in Table 4 can be used to choose flux wires in accordance with energies of interest. If two wires are chosen such that there are two reactions with threshold neutron energies, the total fluence of the energies between the threshold energies can more reliably measured. In particular, this is important for tests involving graphite or structural materials for advanced-reactor designs, especially in environments for assessing displacements per atom (dpa) damage for 0.1 MeV, 0.5 MeV, 1.0 MeV, etc.

2.3.1 Nominal Flux-Wire Set

For some experiments at the Transient Reactor Test (TREAT) facility and ATR at Idaho National Laboratory, a simple flux-wire package, consisting of Ti, Fe, and Co wires, is employed for reactor dosimetry to assess neutron spectrum. For this work, the number of input files for spectrum unfolding and evaluation of the flux wire selection in conjunction with *a priori* spectrum is exceedingly large. Therefore, it was determined to limit the scope of the spectrum unfolding to data sets that contained at least $(n-1)$ flux wires contained within the {Ti, Fe, Co} set for a set of n flux wires, which reduced the total number of input files for spectrum unfolding to 772, a more-manageable number for which to provide detailed analysis. For example, the flux wire sets {Ti, Au}, {Co, Fe, Ni}, and {Ti, Fe, Co, Nb} are valid; {Au, Ni}, {Co, Ni, Zr}, and {Ti, Fe, Au, Nb} are not.

$$C = \frac{W!}{(W-n)!n!} \quad (1)$$

Table 2. Parameters for Eq. (1).

Variable	Parameter	Value
C	Possible Combinations from W and n	
W	Total Number of Wires Available for Selection	30
n	Number of Selected Wires	2, 3, or 4

Table 3. Chosen cases and number of STAYSL simulations performed.

Case Description	C	Alter Input Spectrum (100-group or 640-group)	Spectrum Adjustment (Normal, Thermal Addition, Thermal Filter)	Degree of Adjustment (Large, Small)	Total Number of Input Files for Spectrum Unfolding
Two Wires	435	2	3	2	5,220
Three Wires	4,060	2	3	2	48,720
Four Wires	27,405	2	3	2	328,860
Total					382,800
Combinations that contain at least $(n-1)$ wire within $\{\text{Co, Fe, Ti}\}$ set for a chosen flux wire package with n wires.					772

Table 4. Materials and Reactions Used for Analysis [4, 16].

Material	Reaction	Approximate Threshold Energy (MeV)	Product Half-Life (sec)
Li	${}^6\text{Li} (\text{n},\alpha) {}^3\text{H}$	-	3.89×10^8
F	${}^{19}\text{F} (\text{n},2\text{n}) {}^{18}\text{F}$	11.5	6586.2
Na	${}^{23}\text{Na} (\text{n},2\text{n}) {}^{22}\text{Na}$	13.2	8.21×10^7
	${}^{23}\text{Na} (\text{n},\gamma) {}^{24}\text{Na}$	-	53989.2
Mg	${}^{24}\text{Mg} (\text{n},\text{p}) {}^{24}\text{Na}$	6	53989.2
Al	${}^{27}\text{Al} (\text{n},\text{p}) {}^{27}\text{Mg}$	3.05	567.48
	${}^{27}\text{Al} (\text{n},\alpha) {}^{24}\text{Na}$	5.87	53989.2
P	${}^{31}\text{P} (\text{n},\text{p}) {}^{31}\text{Si}$	1.54	9438
S	${}^{32}\text{S} (\text{n},\text{p}) {}^{32}\text{P}$	1.7	1232323

Material	Reaction	Approximate Threshold Energy (MeV)	Product Half-Life (sec)
Sc	$^{45}\text{Sc} (\text{n},\gamma) ^{46}\text{Sc}$	-	7239456
Ti	$^{46}\text{Ti} (\text{n},2\text{n}) ^{45}\text{Ti}$	13.7	11088
	$^{46}\text{Ti} (\text{n},\text{p}) ^{46}\text{Sc}$	3	7239456
	$^{47}\text{Ti} (\text{n},\text{p}) ^{47}\text{Sc}$	1.11	289370.9
	$^{48}\text{Ti} (\text{n},\text{p}) ^{48}\text{Sc}$	5.8	157212
V	$^{51}\text{V} (\text{n},\alpha) ^{48}\text{Sc}$	8.1	157212
Mn	$^{55}\text{Mn} (\text{n},\gamma) ^{56}\text{Mn}$	-	9284.04
Fe	$^{54}\text{Fe} (\text{n},2\text{n}) ^{53}\text{Fe}$	14	510.6
	$^{54}\text{Fe} (\text{n},\text{p}) ^{54}\text{Mn}$	1.3	2.70×10^7
	$^{54}\text{Fe} (\text{n},\alpha) ^{51}\text{Cr}$	-	2393366
	$^{56}\text{Fe} (\text{n},\text{p}) ^{56}\text{Mn}$	5.1	9284.04
	$^{58}\text{Fe} (\text{n},\gamma) ^{59}\text{Fe}$	-	3844368
Co	$^{59}\text{Co} (\text{n},2\text{n}) ^{58}\text{Co}$	10.7	6122304
	$^{59}\text{Co} (\text{n},\gamma) ^{60}\text{Co}$	-	1.66×10^8
	$^{59}\text{Co} (\text{n},\alpha) ^{56}\text{Mn}$	6.08	9284.04
Ni	$^{58}\text{Ni} (\text{n},2\text{n}) ^{57}\text{Ni}$	12.7	128160
	$^{58}\text{Ni} (\text{n},\text{p}) ^{58}\text{Co}$	1.2	6122304
	$^{60}\text{Ni} (\text{n},\text{p}) ^{60}\text{Co}$	4.2	1.66×10^8
Cu	$^{63}\text{Cu} (\text{n},2\text{n}) ^{62}\text{Cu}$	11.2	580.38
	$^{63}\text{Cu} (\text{n},\gamma) ^{64}\text{Cu}$	-	45723.6
	$^{63}\text{Cu} (\text{n},\alpha) ^{60}\text{Co}$	4.7	1.66×10^8
	$^{65}\text{Cu} (\text{n},2\text{n}) ^{64}\text{Cu}$	10.2	45723.6
Zn	$^{64}\text{Zn} (\text{n},\text{p}) ^{64}\text{Cu}$	1.6	45723.6
As	$^{75}\text{As} (\text{n},2\text{n}) ^{74}\text{As}$	10.5	1535328
Y	$^{89}\text{Y} (\text{n},2\text{n}) ^{88}\text{Y}$	11.8	9212486
Zr	$^{90}\text{Zr} (\text{n},2\text{n}) ^{89}\text{Zr}$	12.2	282276
Nb	$^{93}\text{Nb} (\text{n},\gamma) ^{94}\text{Nb}$	-	6.41×10^{11}
In	$^{115}\text{In} (\text{n},\gamma) ^{116m}\text{In}$	-	3257.4
I	$^{127}\text{I} (\text{n},2\text{n}) ^{126}\text{I}$	9.25	1117152
La	$^{139}\text{La} (\text{n},\gamma) ^{140}\text{La}$	-	145026.7
Pr	$^{141}\text{Pr} (\text{n},2\text{n}) ^{140}\text{Pr}$	9.6	203.4

Material	Reaction	Approximate Threshold Energy (MeV)	Product Half-Life (sec)
Tm	$^{169}\text{Tm}(\text{n},2\text{n})^{168}\text{Tm}$	8.3	8043840
Ta	$^{181}\text{Ta}(\text{n},\gamma)^{180}\text{Ta}$	-	29354.4
W	$^{186}\text{W}(\text{n},\gamma)^{187}\text{W}$	-	86400
Au	$^{197}\text{Au}(\text{n},2\text{n})^{196}\text{Au}$	8.2	532820.2
	$^{197}\text{Au}(\text{n},\gamma)^{198}\text{Au}$	-	232822.1
Th	$^{232}\text{Th}(\text{n},\gamma)^{233}\text{Th}$	-	1338
U	$^{238}\text{U}(\text{n},\gamma)^{239}\text{U}$	-	1407

2.4 Flux Wire Reaction Rates

For the evaluation of flux-wire combinations, no wires were irradiated as part of this work. The irradiation spectrum was simulated, and reaction rates were calculated from the MCNP results and the IRDFF cross-section library for each wire's reaction. For each wire, the irradiation environment and, therefore, reaction rate were not altered. Instead, the *a priori* guess was altered. To avoid the issue of transmutation of isotopes during an extended irradiation similar to HFIR or ATR, the simulation was purported to have occurred over one second, so the daughter isotopes from each wire reaction did not have the neutron fluence to effectively change their concentration beyond the initial production term. Additionally, because the reaction rates were simulated, no complications are provided by thickness of the wire material, where isotopes near the center of a wire experience local flux changes in magnitude or energy.

The production mechanism follows Bateman production-depletion equations, shown in Eq. (2) and (3). The solution for the daughter isotope—i.e., activation product in the flux wire—is shown in Eq. (4). If depletion of the isotopes during irradiation is small ($\sigma\phi < \lambda$), Eq. (4) may be reduced to Eq. (5). By rearranging and combining terms, an expression for the reaction rate of the parent to produce the daughter isotope can be derived in Eq. (6) and Eq. (7). Because the cross-section is dependent on neutron energy, the final form of Eq. (8) may be used to determine the reaction rate by Riemann sums of the production cross-section, multiplied by the neutron flux, which is the same expression that appears in [1]. All the variables used in Eq. (2) through Eq. (8) are defined in Table 5. The reaction rates used for each spectrum unfolding were calculated with Eq. (8) from the HFIR PT-1 neutron spectrum and the chosen flux wires with their respective parent and activation products.

$$\frac{dN_P}{dt} = -\sigma_{t_p}\phi N_P \quad (2)$$

$$\frac{dN_D}{dt} = -(\sigma_{t_D}\phi + \lambda_D)N_D + \sigma_{P \rightarrow D}\phi N_P \quad (3)$$

$$N_D = N_{D,0}e^{-(\sigma_{t_D}\phi + \lambda_D)t} + \frac{\sigma_{P \rightarrow D}\phi N_{P,0}}{\sigma_{t_D}\phi + \lambda_D - \sigma_{t_p}\phi} \left(e^{-\sigma_{t_p}\phi t} - e^{-(\sigma_{t_D}\phi + \lambda_D)t} \right) \quad (4)$$

$$N_D = \frac{\sigma_{P \rightarrow D}\phi N_{P,0}}{\lambda_D} \left(1 - e^{-\lambda_D t} \right) \quad (5)$$

$$\frac{\lambda_D N_{D,\infty}}{N_{P,0}} = \sigma_{P \rightarrow D} \phi \quad (6)$$

$$R(E_i) = \frac{\lambda_D N_{D,\infty}|_{\phi=E_i}}{N_{P,0}} = \sigma_{P \rightarrow D}(E_i) \phi(E_i) \quad (7)$$

$$R = \frac{\lambda_D N_{D,\infty}}{N_{P,0}} = \int_0^{\infty} \sigma_{P \rightarrow D}(E) \phi(E) dE = \sum_{i=1}^I \sigma_{P \rightarrow D}(E_i) \phi(E_i) \quad (8)$$

Table 5. Definition of variables for calculation of reaction rate from simulated data.

Variable	Definition
N	Number of isotopes
P	Parent
D	Daughter
t	Time (sec)
ϕ	Neutron Flux (n/cm ² /sec)
λ	Decay Constant (sec ⁻¹)
$\sigma_{P \rightarrow D}$	Production cross section from parent to daughter
σ_t	Total removal cross section
R	Reaction Rate (sec ⁻¹)
E	Energy

2.5 Spectrum Unfolding Algorithm – STAYSL

For this work, familiarity with the spectrum-unfolding code STAYSL PNNL was leveraged to assess the ability for STAYSL to unfold the “true” spectrum used to calculate flux-wire reaction rates from the neutron spectrum that was provided as an input spectrum, some of which had small or large deviations from the nominal MCNP spectrum.

A brief description of available neutron-spectrum adjustment and unfolding codes may be found in [3]. Additionally, ASTM Standard E944 [3] provides Eq. (9) as an illustration for how STAYSL calculates the adjusted groupwise fluences (Φ'), with the variables defined in Table 6. Eq. (9) provides a nonlinear equation with covariance data for several variables, preventing the analytical assessment of flux-wire selection’s impact and mandating the use of test cases to perform the evaluation.

$$\Phi' - \Phi_0 = C_{\Phi_0} S_{\Phi_0}^T \left(S_{\Phi_0} C_{\Phi_0} S_{\Phi_0}^T + S_{\Sigma_0} C_{\Sigma_0} S_{\Sigma_0}^T + C_{R_m} \right)^{-1} (R_m - R_0) \quad (9)$$

Table 6. Definition of variables for spectral adjustment [1].

Variable	Definition
Φ'	Column vector of the adjusted groupwise fluences
Φ_0	Column vector of the prior spectrum fluences
C_{Φ_0}	Covariance matrix of prior spectrum
S_{Φ_0}	Matrix of sensitivities of the calculated responses to the prior fluences
S_{Σ_0}	Matrix of sensitivities of the calculated responses to the response functions
C_{Σ_0}	Covariance matrix of the response functions
C_{R_m}	Covariance matrix of the measured responses
R_m	Column vector of the measured responses
R_0	Column vector of the responses calculated using the prior spectrum and response functions
Superscript T	Transpose of the matrix
Superscript -1	Inverse of the matrix

2.6 Comparison of Experimentally adjusted Neutron Flux

Finally, the comparison of the experimentally adjusted neutron flux to the input spectrum must be executed. In this work, the input spectrum is known since the flux wire reaction rates were calculated from a simulated true spectrum. The comparison essentially closes the loop, as shown in Figure 1. With real irradiated wires, this direct group-to-group comparison between the *a priori* and experimentally adjusted spectra can help inform discrepancies in a computational model and/or future flux wire choices in additional experiments.

3. RESULTS AND DISCUSSION

The results in Table 7 and Table 8 show the wire combinations that result in all three cases: 100-group with small deviation, 640-group with large deviation, and 640-group with small deviation being within 25% of the cumulative χ^2 of the {Ti, Fe, Co} set. Because this is the nominal case, all flux-wire combinations are compared to this wire set. Note that the 100-group, large-deviation case is not considered. There were no acceptable unfolded spectra with a coarse, large-error *a priori* spectrum. Recall that small deviations are approximately 5% different from the irradiated spectrum at 1 MeV, and large deviations are approximately 50% different from the irradiation spectrum at 1 MeV.

Table 7. Results for potentially large deviation in *a priori* spectrum.

Successful wire combinations for: 100-group with Small Deviation, 640-group with Large Deviation, 640-group with Small Deviation			
Wire #1	Wire #2	Wire #3	Wire #4
Ti	Fe	Co	
Fe	Au		
Fe	Co		
Fe	Cu		
Ti	Fe		
F	Ti	Fe	
Fe	Co	Au	
Fe	Co	Zn	
Li	Ti	Fe	
Mg	Ti	Fe	
Na	Ti	Fe	
P	Ti	Fe	
S	Fe	Co	
S	Ti	Fe	
Ti	Fe	As	
Ti	Fe	Au	
Ti	Fe	Cu	
Ti	Fe	I	
Ti	Fe	In	
Ti	Fe	Nb	
Ti	Fe	Pr	
Ti	Fe	Ta	
Ti	Fe	Tm	
Ti	Fe	Y	
Ti	Fe	Zn	
Ti	Fe	Zr	
Ti	Mn	Fe	
Ti	V	Fe	
Mg	Ti	Fe	Co
Na	Ti	Fe	Co
S	Ti	Fe	Co
Ti	Fe	Co	Au
Ti	Fe	Co	I
Ti	Fe	Co	La

Table 8. Results for well-characterized, high-confidence *a priori* spectrum.

Successful wire combinations for: 100-group with Small Deviation, 640-group with Small Deviation			
Wire #1	Wire #2	Wire #3	Wire #4
Ti	Fe	Co	
Co	U		
Co	In		
Co	La		
Co	Th		
Fe	Au		
Fe	Co		
Fe	Cu		
Li	Co		
S	Co		
Ti	Fe		
Al	Ti	Fe	
F	Ti	Fe	
Fe	Co	Au	
Fe	Co	Nb	
Fe	Co	Zn	
Li	Ti	Fe	
Mg	Ti	Fe	
Na	Ti	Fe	
P	Ti	Fe	
S	Fe	Co	
S	Ti	Fe	
Ti	Fe	As	
Ti	Fe	Au	
Ti	Fe	Cu	
Ti	Fe	I	
Ti	Fe	In	
Ti	Fe	La	
Ti	Fe	Nb	
Ti	Fe	Pr	
Ti	Fe	Ta	
Ti	Fe	Tm	
Ti	Fe	Y	
Ti	Fe	Zn	
Ti	Fe	Zr	
Ti	Mn	Fe	
Ti	V	Fe	
Al	Ti	Fe	Co
F	Ti	Fe	Co
Mg	Ti	Fe	Co
Na	Ti	Fe	Co
P	Ti	Fe	Co
S	Ti	Fe	Co

Successful wire combinations for: 100-group with Small Deviation, 640-group with Small Deviation			
Wire #1	Wire #2	Wire #3	Wire #4
Ti	Fe	Co	As
Ti	Fe	Co	Au
Ti	Fe	Co	I
Ti	Fe	Co	La
Ti	Fe	Co	Nb
Ti	Fe	Co	Y
Ti	Fe	Co	Zr
Ti	Mn	Fe	Co

Figure 3 and Figure 4 provide spectrum-unfolding solutions from STAYSL with Co and Au and Co and Al, respectively. In each plot, the original flux is shown in blue, which is the spectrum used to calculate the reaction rates of the wire reactions, and the other three lines are the STAYSL-adjusted spectra for the nominal, unchanged flux in red, the increased thermal flux in yellow, and the decreased thermal flux (or increased fast flux) in purple. Refer back to Figure 2 for the concept of the adjusted input, *a priori* neutron spectra.

In Figure 3, for the Co and Au flux-wire combination, all the STAYSL-adjusted spectra are indistinguishable from each other, despite their different *a priori* spectra, and they are fairly close to the original flux used for the wires' reaction-rate calculations.

In Figure 4, for the Co and Al flux-wire combination, there are definitive differences in each of the STAYSL-adjusted spectra, and these deviate from the original flux. This wire combination fails to achieve a good agreement with the original flux because of the flux wire's reaction cross-section. The pairing of Co and Al cannot handle an *a priori* spectrum that is not close to the true original spectrum.

Therefore, Co-Au is determined to be an acceptable flux wire combination under the conditions of 640-group, small deviation *a priori* spectrum, and Co-Al is deemed to be an unacceptable pair.

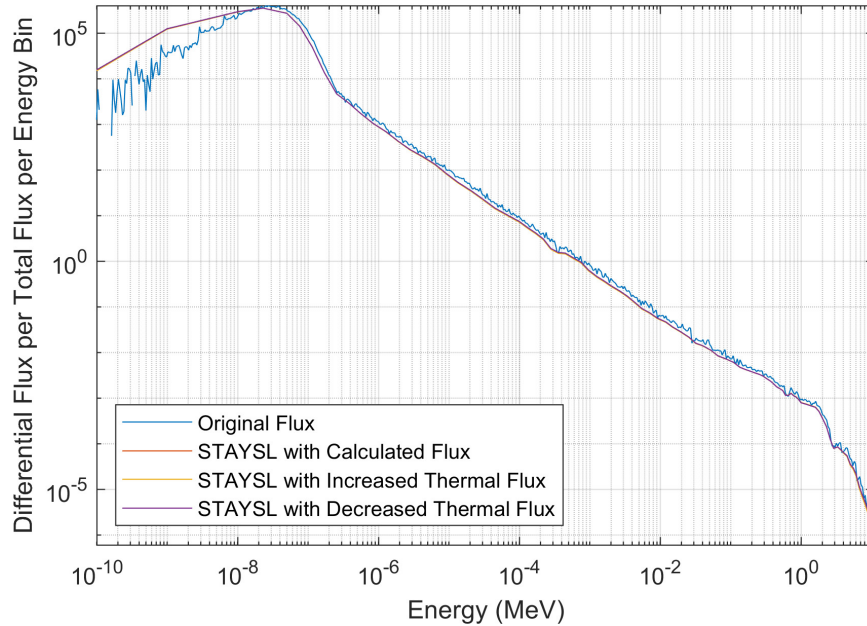


Figure 3. Spectrum unfolding for Co and Au with 640-group, small deviation *a priori* spectrum.

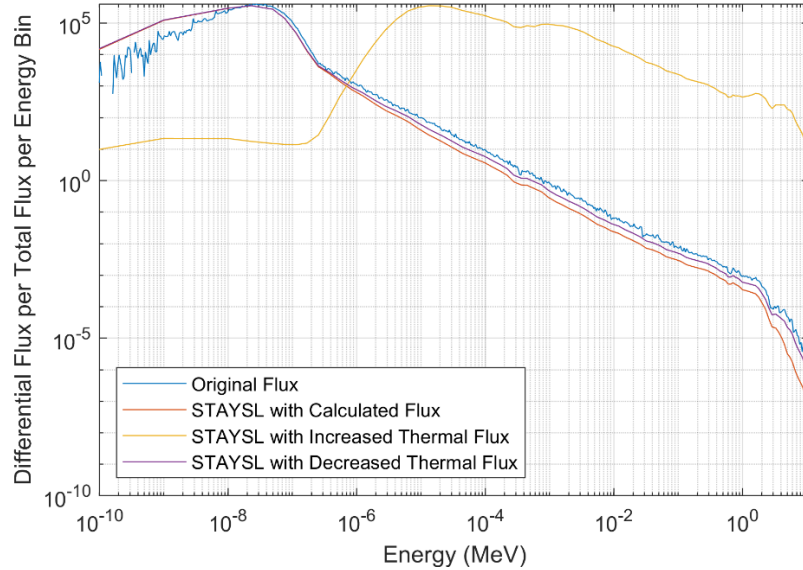


Figure 4. Spectrum unfolding for Co and Al with 640-group, small deviation *a priori* spectrum.

3.1 Potential Large Deviation in *a priori* Spectrum

For a potentially large deviation in the *a priori* spectrum, such as an poorly characterized or uncharacterized irradiation position in the reactor, the list of wires in Table 7 is satisfactorily comparable to the {Ti, Fe, Co} wire set. Because any combinations will be satisfactory, it may be of interest to compare the threshold energy reactions in Table 4 with the wire sets in Table 7 to use energy thresholds related to the expected neutron energies that cause damage, dislocations, or displacement in an experiment. Table 7 is not an exhaustive list, and for other facilities or irradiation positions, analyses could be performed to produce a similar list, but without the requirement of the {Ti, Fe, Co} data set.

However, if the flux wires are located in an uncharacterized or poorly characterized irradiation position in the reactor, it is best practice to prepare an *a priori* spectrum with many neutron energy groups to ensure that the wire choices have the best opportunity to obtain an unfolded spectrum insensitive to errors in the groupwise *a priori* spectrum.

3.2 Well-Characterized, High-Confidence *a priori* Spectrum

Expanding upon Table 7, Table 8 provides the list of flux-wire combinations that may be used to unfold the irradiation spectrum successfully (as well as Ti, Fe, Co) if the *a priori*, simulated spectrum is well-characterized and close to the true irradiation spectrum, providing confidence in the simulated spectrum.

Well-characterized is a completely generic term and should not be used without a caveat that states that it is a generic term. Nevertheless, if an experiment is placed in an irradiation position that has been characterized previously and already has an experimentally adjusted spectrum associated with it, slight changes in the irradiation position or spectrum can be investigated with the wire combinations shown in Table 8, which does contain all the wire combinations found in Table 7. Table 8 is not an exhaustive list, and additional analyses could be performed for other facilities or irradiation positions to produce a similar list, but without the requirement of the {Ti, Fe, Co} data set.

The advantage of the well-characterized, high-confidence wire combinations in Table 8 is the increased number of wires that may be implemented with confidence in the unfolded spectrum. Therefore, by comparing Table 4 and Table 8, more detailed fast energy groups may be evaluated when slight changes in the irradiation spectrum occur.

4. REFERENCES

1. ASTM, *Standard Guide for Determining Neutron Energy Spectra from Neutron Sensors for Radiation-Hardness Testing of Electronics*, ASTM Standard Designation E721-16.
2. ASTM, *Standard Practice for Characterizing Neutron Fluence Spectra in Terms of an Equivalent Monoenergetic Neutron Fluence for Radiation-Hardness Testing of Electronics*, ASTM Standard Designation E722-19.
3. ASTM, *Standard Guide for Application of Neutron Spectrum Adjustment Methods in Reactor Surveillance*, ASTM Standard Designation E944-19.
4. A. Trkov, et al., *IRDF-II: A New Neutron Metrology Library*, Special Issues of Nuclear Data Sheets (163), p. 1-108, 2020.
5. L. R. Greenwood and C. D. Johnson, *User Guide for the STAYSL PNNL Suite of Software Tools*, PNNL-22253, February 2013.
6. E. Ashbaker, *Characterizing the Neutron Spectra in Various Irradiation Facilities within the Oregon State University TRIGA Reactor*, Thesis, 2005.
7. P. J. Griffin, J. G. Kelly, and J. W. VanDenburg, *User's Manual for SNL-SAND-II Code*, SAND 93-3957, April 1994.
8. V. K. Patel, *Novel Uncertainty Quantification Method for Computational Reactor Design Analysis of Nuclear Thermal Propulsion Cores*, Dissertation, 2019.
9. V. Patel, et al., *An Uncertainty Quantification Method Relevant to Material Test Reactors*, Annals of Nuclear Energy, In Review.
10. E. L. MacConnachie and D. R. Novog, Measurement, Simulation, and Uncertainty Quantification of the Neutron Flux at the McMaster Nuclear Reactor, Annals of Nuclear Energy 151, 2021.
11. V. Radulovic, et al., Characterization of the Neutron Spectra in Three Irradiation Channels of the JSI TRIGA Reactor using the GRUPINT Spectrum Adjustment Code, Nuclear Data Sheets 167, 2020: 61–75.
12. D. L. Smith, et al., *Neutron Spectrum Adjustment Using Reaction Rate Data Acquired with a Liquid Dosimetry System*, ANL/TD/CP-90827.
13. D. R. Redhouse, *Uncertainty Quantification of a Genetic Algorithm for Neutron Energy Spectrum Adjustment*, Thesis, 2017.
14. R. M. Vega and E. J. Parma, “Development of a Genetic Algorithm for Neutron Energy Spectrum Adjustment, Joint International Conference on Mathematics and Computation, Supercomputing in Nuclear Applications, and the Monte Carlo Method,” Nashville, TN, April 2015, SAND2015-0298C.
15. K. R. DePriest, *Historical Examination of the ASTM Standard E722 1-MeV Silicon Equivalent Fluence Metric*, SAND 2019-15194, December 2019.
16. D.A.Brown, et al., “ENDF/B-VIII.0: The 8th major release of the nuclear reaction data library with CIELO-project cross sections, new standards and thermal scattering data,” Nuclear Data Sheets (148), 2018.
17. J.T. Goorley, et al., “Initial MCNP6 Release Overview—MCNP6 version 1.0,” LA-UR-13-22934 (2013).

Appendix A

ASTM Standards Relevant to Reactor Dosimetry

Table 9. List of ASTM standards relevant to reactor dosimetry.

Number	Standard Title
D3648	Standard Practices for the Measurement of Radioactivity
D7282	Standard Practice for Set-up, Calibration, and Quality Control of Instruments Used for Radioactivity Measurements
E170	Standard Terminology Relating to Radiation Measurements and Dosimetry
E181	Standard Test Methods for Detector Calibration and Analysis of Radionuclides
E185	Standard Practice for Design of Surveillance Programs for Light-Water Moderated Nuclear Power Reactor Vessels
E261	Standard Practice for Determining Neutron Fluence, Fluence Rate, and Spectra by Radioactivation Techniques
E262	Standard Test Method for Determining Thermal Neutron Reaction Rates and Thermal Neutron Fluence Rates by Radioactivation Techniques
E263	Standard Test Method for Measuring Fast-Neutron Reaction Rates by Radioactivation of Iron
E264	Standard Test Method for Measuring Fast-Neutron Reaction Rates by Radioactivation of Nickel
E265	Standard Test Method for Measuring Reaction Rates and Fast-Neutron Fluences by Radioactivation of S-32
E266	Standard Test Method for Measuring Fast-Neutron Reaction Rates by Radioactivation of Aluminum
E385	Oxygen Content Using a 14-MeV Neutron Activation and Direct-Counting Technique
E393	Standard Test Method for Measuring Reaction Rates by Analysis of Barium-140 from Fission Dosimeters
E481	Standard Test Method for Measuring Neutron Fluence Rates by Radioactivation of Cobalt and Silver
E482	Application of Neutron Transport Methods for Reactor Vessel Surveillance
E496	Measuring Neutron Fluence and Average Energy from $^3\text{H}(\text{d},\text{n})^4\text{He}$ Neutron Generators by Radioactivation Techniques
E521	Investigating the Effects of Neutron Radiation Damage Using Charged-Particle Irradiation
E523	Standard Test Method for Measuring Fast-Neutron Reaction Rates by Radioactivation of Copper
E526	Standard Test Method for Measuring Fast-Neutron Reaction Rates by Radioactivation of Titanium
E531	Surveillance Testing of High-Temperature Nuclear Component Materials
E636	Conducting Supplemental Surveillance Tests for Nuclear Power Reactor Vessels
E666	Calculating Absorbed Dose from Gamma or X Radiation
E668	Application of Thermoluminescence-Dosimetry (TLD) Systems for Determining Absorbed Dose in Radiation-Hardness Testing of Electronic Devices
E693	Standard Practice for Characterizing Neutron Exposures in Iron and Low Alloy Steels in Terms of Displacement Per Atom (dpa)
E704	Standard Test Method for Measuring Reaction Rates by Radioactivation of U-238
E705	Standard Test Method for Measuring Reaction Rates by Radioactivation of Np-237
E706	Light-Water Reactor Pressure Vessel Surveillance Standards
E720	Standard Guide for Selection and Use of Neutron Sensors for Determining Neutron Spectra Employed in Radiation-Hardness Testing of Electronics
E721	Standard Guide for Determining Neutron Energy Spectra from Neutron Sensors for Radiation-Hardness Testing of Electronics
E722	Standard Practice for Characterizing Neutron Fluence Spectra in Terms of Equivalent Monoenergetic Neutron Fluence for Radiation-Hardness Testing of Electronics
E798	Conducting Irradiations at Accelerator-Based Neutron Sources
E821	Measurement of Mechanical Properties During Charged-Particle Irradiation
E844	Standard Guide for Sensor Set Design and Irradiation for Reactor Surveillance

Number	Standard Title
E853	Standard Practice for Analysis and Interpretation of Light-Water Reactor Surveillance Neutron Exposure Results
E854	Standard Test Method for Application and Analysis of Solid State Track Recorder (SSTR) Monitors for Reactor Surveillance
E900	Predicting Radiation-Induced Transition Temperature Shift in Reactor Vessel Materials
E910	Application and Analysis of Helium Accumulation Fluence Monitors for Reactor Vessel Surveillance
E942	Investigating the Effects of Helium in Irradiated Metals
E944	Standard Guide for Application of Neutron Spectrum Adjustment Methods in Reactor Surveillance
E1005	Standard Test Method for Application and Analysis of Radiometric Monitors for Reactor Vessel Surveillance
E1006	Analysis and Interpretation of Physics Dosimetry Results from Test Reactor Experiments
E1018	Standard Guide for Application of ASTM Evaluated Cross Section Data File
E1035	Determining Neutron Exposures for Nuclear Reactor Vessel Support Structures
E1214	Use of Melt Wire Temperature Monitors for Reactor Vessel Surveillance
E1249	Minimizing Dosimetry Errors in Radiation Hardness Testing of Silicon Electronic Devices using Co-60 Sources
E1250	Application of Ionization Chambers to Assess the Low Energy Gamma Component of Cobalt-60 Irradiators Used in Radiation-Hardness Testing of Silicon Electronic Devices
E1297	Standard Test Method for Measuring Fast-Neutron Reaction Rates by Radioactivation of Niobium
E1854	Ensuring Test Consistency in Neutron-Induced Displacement Damage of Electronic Parts
E1855	Use of 2N2222A Silicon Bipolar Transistors as Neutron Spectrum Sensors and Displacement Damage Monitors
E2005	Standard Guide for Benchmark Testing of Reactor Dosimetry in Standard and Reference Neutron Fields
E2006	Benchmark Testing of Light Water Reactor Calculations
E2059	Application and Analysis of Nuclear Research Emulsions for Fast Neutron Dosimetry
E2215	Evaluation of Surveillance Capsules from Light-Water Moderated Nuclear Power Reactor Vessels
E2450	Application of CaF ₂ (Mn) Thermoluminescence Dosimeters in Mixed Neutron-Photon Environments
E2956	Monitoring the Neutron Exposure of LWR Reactor Pressure Vessels
E3063	Test Method for Antimony Content Using Neutron Activation Analysis (NAA)